Toward reconstructing spike trains from large-scale calcium imaging data

Alex C. Kwan[1]

[1]Division of Neurobiology, Department of Molecular and Cell Biology, Helen Wills Neuroscience Institute, University of California, Berkeley, California 94120, USA

(Received 15 December 2009; published online 22 January 2010)

Neural activity can be captured by state-of-the-art optical imaging methods although the analysis of the resulting data sets is often manual and not standardized. Therefore, laboratories using large-scale calcium imaging eagerly await software toolboxes that can automate the process of identifying cells and inferring spikes. An algorithm proposed and implemented in a recent paper by Mukamel *et al.* [*Neuron* 63, 747–760 (2009)] used independent component analysis and offers significant improvements over conventional methods. The approach should be widely applicable, as tested with data obtained from the mouse cerebellum, neocortex, and spinal cord. The emergence of analysis tools in parallel with the rapid advances in optical imaging is an exciting development that will stimulate new discoveries and further elucidate the functions of neural circuits. [DOI: 10.2976/1.3284977]

CORRESPONDENCE
Alex C. Kwan:
alexkwan@berkeley.edu

Spikes are the language of the brain and the means by which neurons communicate. A precise, quantitative description of spike trains from a single sensory neuron can tell us about how the external world may be encoded by neural activity (Rieke *et al.*, 1996). However, neurons do not work alone. Simultaneous recordings of many neurons will let us verify intuitions extrapolated from single-neuron studies and develop population models. Exploring such population code with multi-electrode recording has led to exciting insights on the encoding strategies employed by neuronal populations (Mazor and Laurent, 2005; Pillow *et al.*, 2008).

Large-scale calcium imaging is an emerging approach for measuring population neural activity at single cell resolution (Kerr and Denk, 2008). Spikes can be inferred by an increase in intracellular calcium, which is optically probed with fluorescent calcium indicators. Visualization of large neuronal populations *in vivo* is made possible by multicell bolus loading of inorganic dyes (Stosiek *et al.*, 2003) or viral injection of genetically engineered proteins. Although deep-tissue optical microscopy is slow, it is compatible with fluorescent cell-type markers (Nimmerjahn *et al.*, 2004; Kwan *et al.*, 2009) and can reveal spatial clustering of active neurons (Ohki *et al.*, 2005; Busche *et al.*, 2008). Moreover, genetically encoded calcium indicators allow for functional imaging of the same neurons over weeks (Mank *et al.*, 2008; Tian *et al.*, 2009), opening up opportunities for time-lapse functional plasticity experiments.

Although large-scale calcium imaging has been used in many brain regions and model organisms, suitable and standardized data analysis methods are often not available. At the most basic level, image analysis is a two-step process. First, identify pixels within cell-like structures as a region of interest (ROI). Time-lapse fluorescence traces associated with each ROI are extracted from the raw images. Second, translate the fluorescence changes into spike times or firing rates. For a human operator, the first step is a dull but possible task, whereas a reliable second step is impossible by manual methods, leading to a recent boom in spike inference algorithms. Most of these algorithms rely on the fact that somatic fluorescence change due to a single spike is filtered by a slower exponential decay function. One method, template-matching and deconvolution (Kerr *et al.*, 2005; Yaksi and Friedrich,

2006), works well for sparse activity when interspike intervals are large compared to the fluorescence decay time constant. More sophisticated algorithms (Sasaki *et al.*, 2008; Vogelstein *et al.*, 2009) may address this issue and make spike inference equally reliable for neurons with high firing rates.

Where does this leave the initial step of cell sorting? The fluorescence signal at each pixel can be quite noisy because of shot noise and the usual need for fast imaging frame rate. High basal fluorescence tends to suggest a cell body and sharp signal increase implies neural activity; these are signatures that the human eyes can see but not for simple image segmentation approaches based on binary mask or cross-correlation. This calls for approaches that harness the statistical features unique to large-scale calcium image data sets, such as the algorithm recently proposed and implemented by Mukamel and Nimmerjahn in the laboratory of Schnitzer (Mukamel *et al.*, 2009). The significance of their study is that it completely automates and standardizes the analysis portion, from fluorescence to spike trains, of large-scale calcium imaging experiments.

A QUANTITATIVE APPROACH FOR AUTOMATIC CELL SORTING

The key insight of Mukamel *et al.* was that the spatial and temporal characteristics of large-scale calcium imaging data sets can be used to find the locations of cells. Regions likely to be cells would contain groups of neighboring pixels with fluorescence intensities that are different from the rest of the image; therefore there is a spatial sparseness. Moreover, spikes are accompanied by large, distinct fluorescence peaks occurring at only certain image frames, leading to a temporal sparseness.

The goal then becomes identifying the regions that satisfy these sparseness criteria and the algorithm of Mukamel *et al.* uses independent component analysis (ICA). A simple way to think about ICA is to consider the cocktail party problem where there is only one set of ears (detectors) and many conversations going on (signal and noise sources). How do you unmix the sound to retrieve the true signal? Assuming that each detector is sensing a weighted sum of independent signal and noise sources, ICA untangles the problem and provides an optimal estimate of the various sources (Bell and Sejnowski, 1995; Hyvärinen and Oja, 2000). In neuroscience, ICA has been used theoretically to argue for a sparse coding scheme for encoding natural images (Olshausen and Field, 1996; Bell and Sejnowski, 1997). Practically, ICA can isolate components of brain activity from multisite electroencephalography (EEG) recordings (Makeig *et al.*, 1997).

One shortcoming of ICA is that the algorithm does not know the number of signal sources and is prone to error when many detectors are present. Mukamel's algorithm got

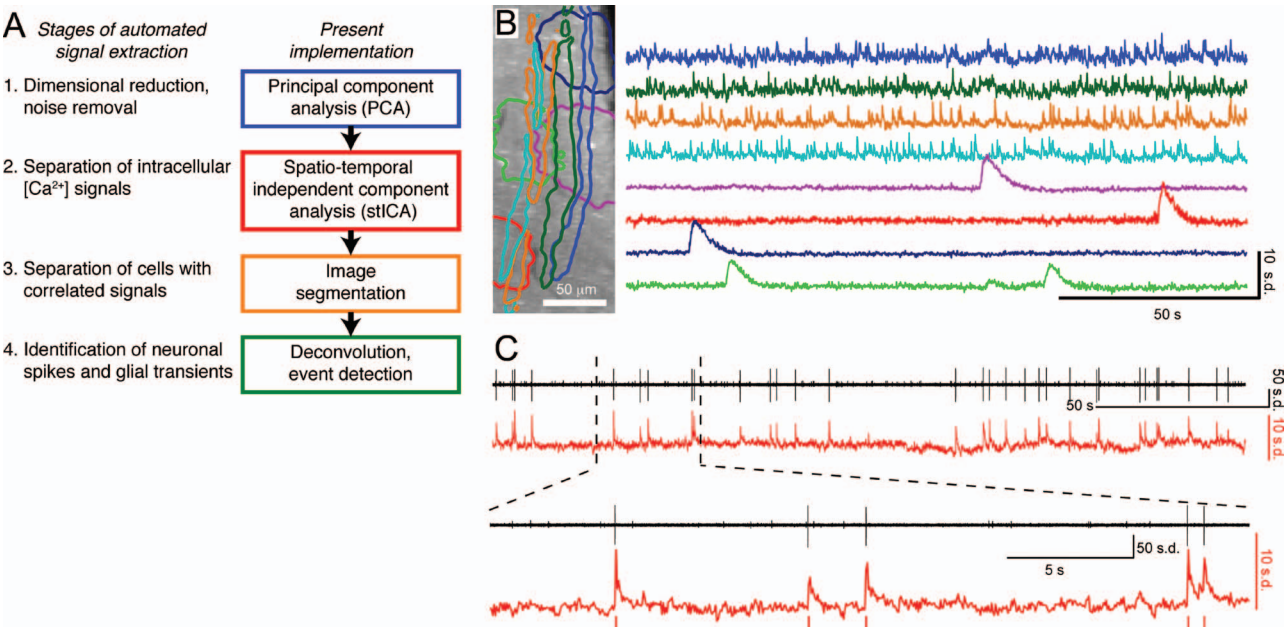

Figure 1. Automated cell sorting and spike train reconstruction from large-scale calcium imaging data. (A) The workflow of the automated analysis algorithm proposed and implemented by Mukamel *et al.* (2009). (B) From calcium imaging data recorded in the mouse cerebellum *in vivo*, the algorithm automatically selected spatial and temporal filter pairs with morphologies and transients expected for individual Purkinje dendrites and Bergmann glia. (C) Simultaneous calcium imaging and single-unit recording confirmed that the extracted fluorescence transients correlated well with spike trains recorded from the two cell types. [Reprinted from Mukamel *et al.* (2009), with permission from Elsevier].

around this problem by starting with a principal component analysis (PCA) step. The PCA, by finding and retaining only the spatiotemporal components that exhibit the largest variance, reduces the dimensionality of the data set prior to the ICA. Furthermore, if neural activity is correlated, ICA can lump together regions containing multiple cells, so a post-ICA segmentation step was added to split spatially disjoint independent components. These three steps plus a template-matching spike inference step formed the basis for the automated image analysis of Mukamel *et al.* [Fig. 1(A)].

ALGORITHM APPLIED TO REAL DATA SETS

How well does the ICA algorithm of Mukamel *et al.* work? Using the data from imaging the cerebellum of running, head-restrained mice (Nimmerjahn *et al.*, 2009), the algorithm was able to identify the regions that correspond to Purkinje dendrites and Bergmann glia [Fig. 1(B)]. This was an impressive feat because unlike in the neocortex, the cerebellar structures are overlapping and have low basal fluorescence [see the Supplementary Movies in Nimmerjahn *et al.* (2009)]. The sorted regions had clean and distinct calcium transients with clear electrophysiological correlates [Fig. 1(C)]. To quantify the effectiveness of the algorithm, Mukamel *et al.* varied two variables in simulated data: the signal-to-noise ratio and the number of cells. In most cases, ICA outperformed manual ROI analysis. However, in extreme cases where the signal-to-noise ratio is very low (<0.1) or when there are too many cells (>200), errors of the ICA algorithm could suddenly increase.

One significant benefit of ICA is that noise sources are treated as independent components, even if they share the same pixels as the signal sources. As a result, motion artifacts in the extracted fluorescence signals were mitigated. This will be increasingly useful as calcium imaging moves toward *in vivo* experiments in awake animals (Dombeck *et al.*, 2007; Flusberg *et al.*, 2008; Murayama *et al.*, 2009; Sawinski *et al.*, 2009). More importantly, spatially overlapping Purkinje dendrites and Bergmann glia in the cerebellum can be identified as separate signal sources [Fig. 1(B)]. In other cases, when overlapping is undesirable, such as when neuropil is contaminating somatic fluorescence signals in the neocortex, ICA can better estimate the true signals.

A good algorithm should be applicable to imaging data sets obtained from other brain regions. For this purpose, I tried the ICA algorithm, generously provided as Supplementary Materials in Mukamel *et al.* (2009), on data obtained from neocortex and spinal cord imaging experiments. The neocortex data were recorded from the visual cortex of anesthetized mice [Alitto and Dan (2009), unpublished data] and contained cells with highly correlated activity. The ICA algorithm was able to automatically identify $>90\%$ of the active cortical cells [Fig. 2(A)], although it missed a few cells with low basal fluorescence or ultrasparse activity. The mouse spinal cord data posed a greater challenge: spinal interneurons had high firing rates during fictive locomotion induced by neurotransmitters (Kwan *et al.*, 2009). Even in this case where the temporal sparseness condition was likely untrue, the algorithm managed to identify a subset of the active neurons [Fig. 2(B)].

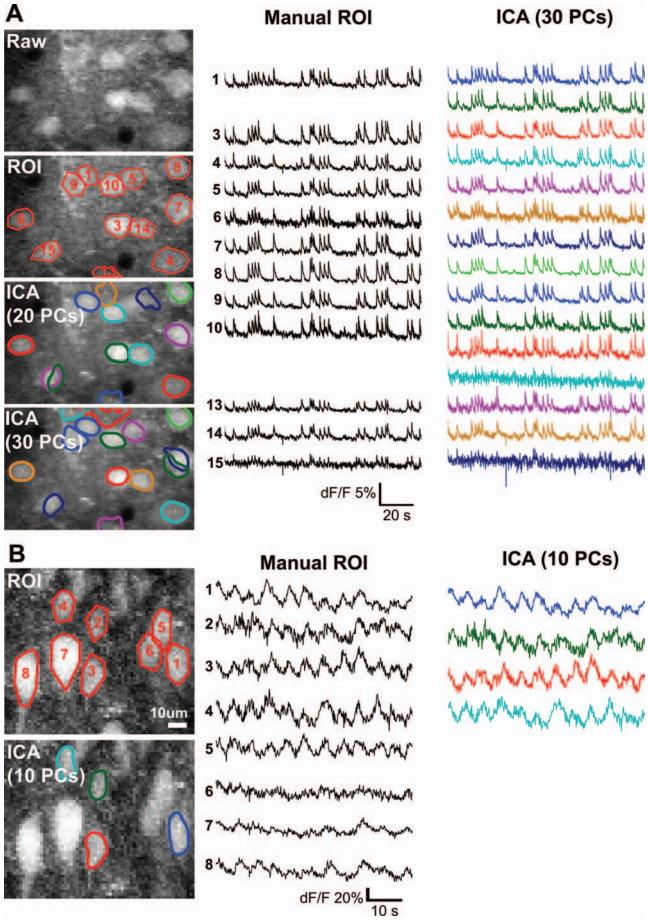

Figure 2. Automated cell sorting applied to data from the mouse neocortex and spinal cord. (A) The data set consists of 1000 time-lapse image frames of neocortical cells labeled via multicell bolus loading [H Alitto and Y Dan (2009), unpublished data]. Cell bodies were initially identified manually as ROIs. In most cases, the ICA algorithm identified $>90\%$ of the cell in the field of view, although sometimes ICA missed cells with low basal fluorescence or very sparse activity. Moreover, the set of cells selected by the ICA algorithm could vary slightly depending on the number of principal components used. (B) Spinal interneurons were rhythmically bursting during fictive locomotion in mouse spinal cord. The ICA algorithm was able to pick up a subset of the interneurons that have the largest fluorescence changes.

CHALLENGES AND OUTLOOK

In the current algorithm, the detected set of cell locations can depend on the initial parameters such as the number of principal components used [Fig. 2(A)]. The consistency

Table I. Some algorithms used for analyzing large-scale calcium imaging data.

Usage	Principle	References
Automated cell sorting	Cross-correlation	Ozden *et al.* (2008)
	Independent component analysis	Mukamel *et al.* (2009)
Spike inference	Template-matching filters and deconvolution	Kerr *et al.* (2005), Yaksi and Friedrich (2006), and Greenberg and Kerr (2009)
	Clustering	Sato *et al.* (2007)
	Supervised learning	Sasaki *et al.* (2008)
	Particle filter	Vogelstein *et al.* (2009)
Motion correction	Hidden Markow chains	Dombeck *et al.* (2007)
	Lucas–Kanade	Greenberg and Kerr (2009)
	Multiresolution nonlinear least-square optimization	Thevenaz *et al.* (1998) and TurboReg plug-in for ImageJ

seems to improve for images with small field of view, which agrees with the calculation by Mukamel *et al.* of fidelity as a function of the number of cells. This trend suggests a possible strategy of breaking the field of view into smaller parts and recombining following ICA. The ICA algorithm would operate in a stable regime and fidelity could be further improved by checking that the same cells are sorted from redundant, smaller images.

A general concern for large-scale calcium imaging is that the spikes or firing rates are inferred and not directly measured. Combined imaging and electrophysiological measurements have shown that in most experiments, somatic calcium is directly related to spiking activity (Kerr *et al.*, 2005; Sato *et al.*, 2007; Kwan *et al.*, 2009; Mukamel *et al.*, 2009; Tian *et al.*, 2009) but in certain cases this spike-calcium relationship may not hold true (Lin *et al.*, 2007; Moreaux and Laurent, 2007). Some of the unexpected fluorescence signals could be due to neuropil contamination, which would be reduced by employing the ICA algorithm. Nonetheless, when experimenting in new biological contexts, the spike-calcium relationship must be validated.

In spite of some minor issues, the ICA algorithm of Mukamel *et al.* represents an important step toward the reconstruction of multicell spike trains from large-scale calcium imaging data. In the next few years, complete software toolboxes including cell sorting and spike inference algorithms (Table I) should provide a one-stop solution for the imaging community. A standardized analysis framework will enable fast and reliable optical readout of multineuron activity, further making the case for optical imaging to be a preferred method for cracking the neural code.

ACKNOWLEDGMENTS

A.C.K. is supported by a Croucher Foundation Fellowship. The author thanks Aaron Kaluszka and Henry Alitto for the insightful discussions.

REFERENCES

Bell, AJ, and Sejnowski, TJ (1995). "An information maximization approach to blind separation and blind deconvolution." *Neural Comput.* **7**, 1129–1159.

Bell, AJ, and Sejnowski, TJ (1997). "The 'independent components' of natural scenes are edge filters." *Vision Res.* **37**, 3327–3338.

Busche, MA, Eichhoff, G, Adelsberger, H, Abramowski, D, Wiederhold, KH, Haass, C, Staufenbiel, M, Konnerth, A, and Garaschuk, O (2008). "Clusters of hyperactive neurons near amyloid plaques in a mouse model of Alzheimer's disease." *Science* **321**, 1686–1689.

Dombeck, DA, Khabbaz, AN, Collman, F, Adelman, TL, and Tank, DW (2007). "Imaging large-scale neural activity with cellular resolution in awake, mobile mice." *Neuron* **56**, 43–57.

Flusberg, BA, Nimmerjahn, A, Cocker, ED, Mukamel, EA, Barretto, RPJ, Ko, TH, Burns, LD, Jung, JC, and Schnitzer, MJ (2008). "High-speed, miniaturized fluorescence microscopy in freely moving mice." *Nat. Methods* **5**, 935–938.

Greenberg, DS, and Kerr, JND (2009). "Automated correction of fast motion artifacts for two-photon imaging of awake animals." *J. Neurosci. Methods* **176**, 1–15.

Hyvärinen, A, and Oja, E (2000). "Independent component analysis: algorithms and applications." *Neural Networks* **13**, 411–430.

Kerr, JND, and Denk, W (2008). "Imaging *in vivo*: watching the brain in action." *Nat. Rev. Neurosci.* **9**, 195–205.

Kerr, JND, Greenberg, D, and Helmchen, F (2005). "Imaging input and output of neocortical networks *in vivo*." *Proc. Natl. Acad. Sci. U.S.A.* **102**, 14063–14068.

Kwan, AC, Dietz, SB, Webb, WW, and Harris-Warrick, RM (2009). "Activity of Hb9 interneurons during fictive locomotion in mouse spinal cord." *J. Neurosci.* **29**, 11601–11613.

Lin, BJ, Chen, TW, and Schild, D (2007). "Cell type-specific relationships between spiking and [Ca2+](i) in neurons of the Xenopus tadpole olfactory bulb." *J. Physiol. (London)* **582**, 163–175.

Makeig, S, Jung, TP, Bell, AJ, Ghahremani, D, and Sejnowski, TJ (1997). "Blind separation of auditory event-related brain responses into independent components." *Proc. Natl. Acad. Sci. U.S.A.* **94**, 10979–10984.

Mank, M, Santos, AF, Direnberger, S, Mrsic-Flogel, TD, Hofer, SB, Stein, V, Hendel, T, Reiff, DF, Levelt, C, Borst, A, Bonhoeffer, T, Hubener, M, and Griesbeck, O (2008). "A genetically encoded calcium indicator for chronic *in vivo* two-photon imaging." *Nat. Methods* **5**, 805–811.

Mazor, O, and Laurent, G (2005). "Transient dynamics versus fixed points in odor representations by locust antennal lobe projection neurons." *Neuron* **48**, 661–673.

Moreaux L, and Laurent G (2007). "Estimating firing rates from calcium signals in locust projection neurons in *in vivo*." Frontiers in Neural Circuits 1.

Mukamel, EA, Nimmerjahn, A, and Schnitzer, MJ (2009). "Automated analysis of cellular signals from large-scale calcium imaging data." *Neuron* **63**, 747–760.
Murayama, M, Perez-Garci, E, Nevian, T, Bock, T, Senn, W, and Larkum, ME (2009). "Dendritic encoding of sensory stimuli controlled by deep cortical interneurons." *Nature (London)* **457**, 1137–1141.
Nimmerjahn, A, Kirchhoff, F, Kerr, JND, and Helmchen, F (2004). "Sulforhodamine 101 as a specific marker of astroglia in the neocortex *in vivo*." *Nat. Methods* **1**, 31–37.
Nimmerjahn, A, Mukamel, EA, and Schnitzer, MJ (2009). "Motor behavior activates Bergmann glial networks." *Neuron* **62**, 400–412.
Ohki, K, Chung, S, Ch'ng, YH, Kara, P, and Reid, RC (2005). "Functional imaging with cellular resolution reveals precise micro-architecture in visual cortex." *Nature (London)* **433**, 597–603.
Olshausen, BA, and Field, DJ (1996). "Emergence of simple-cell receptive field properties by learning a sparse code for natural images." *Nature (London)* **381**, 607–609.
Ozden, I, Lee, HM, Sullivan, MR, and Wang, SSH (2008). "Identification and clustering of event patterns from *in vivo* multiphoton optical recordings of neuronal ensembles." *J. Neurophysiol.* **100**, 495–503.
Pillow, JW, Shlens, J, Paninski, L, Sher, A, Litke, AM, Chichilnisky, EJ, and Simoncelli, EP (2008). "Spatio-temporal correlations and visual signalling in a complete neuronal population." *Nature (London)* **454**, 995–999.
Rieke, F, Warland, D, de Ruyter van Steveninck, RR, and Bialek, W (1996). *Spikes: exploring the neural code*, MIT Press, Cambridge, MA.
Sasaki, T, Takahashi, N, Matsuki, N, and Ikegaya, Y (2008). "Fast and accurate detection of action potentials from somatic calcium fluctuations." *J. Neurophysiol.* **100**, 1668–1676.
Sato, TR, Gray, NW, Mainen, ZF, and Svoboda, K (2007). "The functional microarchitecture of the mouse barrel cortex." *PLoS Biol.* **5**, e189.
Sawinski, J, Wallace, DJ, Greenberg, DS, Grossmann, S, Denk, W, and Kerr, JND (2009). "Visually evoked activity in cortical cells imaged in freely moving animals." *Proc. Natl. Acad. Sci. U.S.A.* **106**, 19557–19562.
Stosiek, C, Garaschuk, O, Holthoff, K, and Konnerth, A (2003). " *In vivo* two-photon calcium imaging of neuronal networks." *Proc. Natl. Acad. Sci. U.S.A.* **100**, 7319–7324.
Thevenaz, P, Ruttimann, UE, and Unser, M (1998). "A pyramid approach to subpixel registration based on intensity." *IEEE Trans. Image Process.* **7**, 27–41.
Tian, L, Hires, SA, Mao, T, Huber, D, Chiappe, ME, Chalasani, SH, Petreanu, L, Akerboom, J, McKinney, SA, Schreiter, ER, Bargmann, CI, Jayaraman, V, Svoboda, K, and Looger, LL (2009). "Imaging neural activity in worms, flies and mice with improved GCaMP calcium indicators." *Nat. Methods* **6**, 875–881.
Vogelstein, JT, Watson, BO, Packer, AM, Yuste, R, Jedynak, B, and Paninski, L (2009). "Spike inference from calcium imaging using sequential Monte Carlo methods." *Biophys. J.* **97**, 636–655.
Yaksi, E, and Friedrich, RW (2006). "Reconstruction of firing rate changes across neuronal populations by temporally deconvolved Ca2+ imaging." *Nat. Methods* **3**, 377–383.